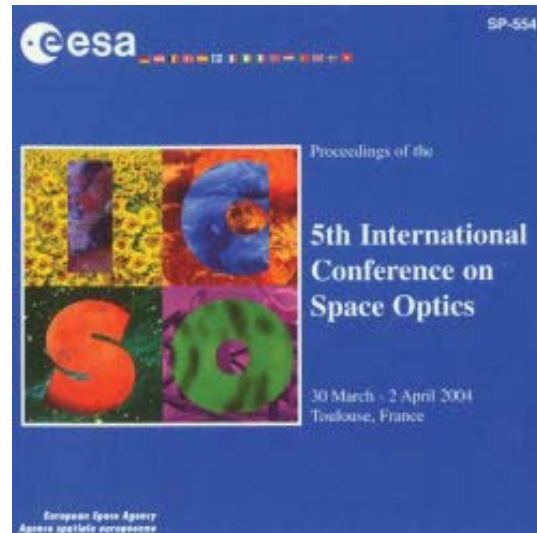


# International Conference on Space Optics—ICSO 2004

Toulouse, France

30 March–2 April 2004

*Edited by Josiane Costeraste and Errico Armandillo*



## *Ageing under mechanical stress: first experiments for a silver based multilayer mirror*

*Arnaud Lalo, Guillaume Ravel, Michel Ignat,  
Bernard Cousin, et al.*



## AGEING UNDER MECHANICAL STRESS: FIRST EXPERIMENTS FOR A SILVER BASED MULTILAYER MIRROR

Arnaud Lalo<sup>(1)</sup>, Guillaume Ravel<sup>(2)</sup>, Michel Ignat<sup>(3)</sup>, Bernard Cousin<sup>(4)</sup>, Michael V Swain<sup>(5)</sup>

<sup>(1)</sup>CNES – DTS/AQ/EQE/AM, 18, av. Éd.-Belin F31055 Toulouse Cedex 4 France, arnaud.lalo@cea.fr

<sup>(2)</sup>CEA – DRT-LETI/DOPT-LTCM, 17, r. des Martyrs F38054 Grenoble Cedex 9 France, ravel@chartreuse.cea.fr

<sup>(3)</sup>LTPCM – CNRS/INPG-ENSEEG, BP75 D.U. F38402 S'-Martin-d'H. France, mignat@ltpcm.inpg.fr

<sup>(4)</sup>CNES – DTS/AQ/EQE/AM, 18, av. Éd.-Belin F31055 Toulouse Cedex 4 France, bernard.cousin@cnes.fr

<sup>(5)</sup>Biomaterials Sc. Unit, Uni. of Sydney, ATP, Eveleigh NSW1430 Australia, mswain@mail.usyd.edu.au

### ABSTRACT

Improving materials and devices reliability is a major concern to the spatial industry. Results are reported for satellite mirrors-like specimens consisting in oxide-protected metal systems. Optical coatings were deposited by electron beam evaporation.

Mechanical stress fields in multi-layered materials play an important role. The stress state can have far-reaching implications both in kinetics and thermodynamics. Therefore an integrated apparatus with four-point bending equipment was designed. The technique allowed us to exert stress into a film or a system of films on a substrate concurrently with thermal treatment. In order to achieve the first tests performed with the help of the apparatus, various preliminary characterizations were required. The article reports the preliminary micro-mechanical testing of the materials (ultra micro-indentation to evaluate the elastic modulus of the samples materials and wafer curvature technique to determine the specimen residual stress) and the first ageing experiment. Experimental evidence of accelerated ageing under stress is successfully reported.

**Keywords:** thin films, ageing, reliability, silver-based mirrors, stress, accelerated life test, nanoindentation, four-point bending

### 1. INTRODUCTION

Satellite integration requires several years imposing that the devices are manufactured a long period beforehand. Afterwards, before the putting into orbit, satellites are likely to stay several months or even years on floor. All this leads to consider materials ageing as a key issue for technological performance.

We are dealing with standard metallic mirrors. These devices typically consist of a superposition of different thin films on a thick low deformation glass:

- a metallic layer promoting adhesion and used as a ground (Ni or Cr),
- a high reflectance metal layer (Ag) and
- an oxide protective layer (SiO<sub>2</sub> or Y<sub>2</sub>O<sub>3</sub>).

#### 1.1. Previous observations of ageing in Ag films

It has long been known that the effect of combined hydrostatic pressure (stress) and uniaxial tension on the rupture time of polycrystalline bulk materials (e.g. copper wire) is of importance [1]. Specimens broke by intergranular fracture due to the growth of voids along grain boundaries under the action of the applied stress (wire under tension). In a given atmosphere (namely, air), this process depends only on stress and pressure.

In the seventies, Presland *et al.* [2,3] focused on hillock formation and voiding by surface diffusion on thin silver films. They observed cavity formation on cooling films (5 Å – 1 μm in thickness) on which hillock had spontaneously been formed. Surface hillock growth was observed by SEM at the first stage in the agglomeration of silver films. This stage was then followed by remaining stages of discrete island formation. This process seemed to be catalysed when the films are deposited onto cadmium sulphide layers or nickel films and in UHV-deposited thin evaporated silver films on exposure to air or oxygen annealing: it was observed that decreasing oxygen partial pressure gives rise to a larger catchment area. It was assumed that oxygen pressure may affect the diffusion coefficient and the critical hole size: in oxygen-containing atmospheres, surface agglomeration occurred rapidly. When annealed in hydrogen atmospheres, the silver films were stable; no change was observed after heating. The rate of hole growth was measured and found to increase with temperature and to attain eventually equilibrium shape.

From a kinetic point of view, hole growth was detected after an induction time, indicating an activation energy. This induction time increased sharply with increased film thickness and decreased as the oxygen partial pressure increased. Stress relief was believed to accompany hillock growth and voiding. The driving force of these phenomena cannot be regarded as surface energy reduction only, as the films have no internal surface area whose reduction could give rise to energy change. Surface hillock formation and subsequent voiding has been associated with

continuous metal films on low thermal expansion substrates (silica glass). The initial stress for silver films deposited on glass substrates at room temperature is tensile and this stress is reduced by removal of material leading to hillock formation and associated voiding. This phenomenon should appear in any atmosphere but in Presland's work, rapid hillock growth was observed only in the presence of oxygen: the increase in the surface self diffusion coefficient by a factor of about 100 x between oxygen-free silver surfaces and oxygen at 760 torr was reported as the main cause.

More recently, a study [4,5] was carried on thicker films at high temperatures (not less than 1000°C). In that case, the metallic underlayer is oxidised by environment oxygen diffusing through the silver film. According to considerations about bonding energy between oxygen and vacancy, oxygen diffusion goes with vacancy diffusion, resulting in vacancy supersaturation as oxidation occurred at the Ag-Ni interface. This vacancy supersaturation at the Ag/NiO/Ni interface condensates into voids which grow towards the surface of the silver film (see Fig. 1). Those holes and the voiding process have been observed by optical techniques. De Monestrol *et al.* pointed out the important role that stress should play on these processes.

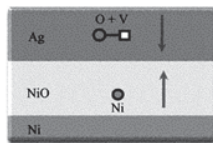


Fig. 1. A schematic diagram of the oxidation and vacancy diffusion supposed to be involved in metal-on-metal ageing. O: oxygen atom; V: vacancy; Ni: nickel atom. (from [4,5])

From an optical point of view, aging histories of optical constants of thermally evaporated silver films have been studied [6]. This study shows that optical constant changes after evaporation of continuous metal films. Preliminary work [7] done at our laboratory showed evidence that protected Ag mirrors undergo some morphological transformations (ageing). Most of them are schematised in Fig. 2: some defects, like pinholes, do not show any evolution (they are probably present since the deposition step), others, like sub-microscopic holes in the Ag layer, do present some temporal evolution. Just after deposition, no holes are detected. Under some circumstances related to materials in contact with Ag, holes are detected after an incubation time.

Careful observations ( see e.g. Fig. 3) allowed us to come to a first conclusion: the holes are unambiguously located in the Ag layer, and their

presence could be related to the state of stress imposed by under and over-layers. In the case of silver mirrors, the ultimate concern is the potential loss of reflectivity coming from mechanical degradation with time. To confirm those first observations, consistent to some extent with literature data, we have to build our own samples, and look at ways to trigger and accelerate ageing by control of external and internal stresses.

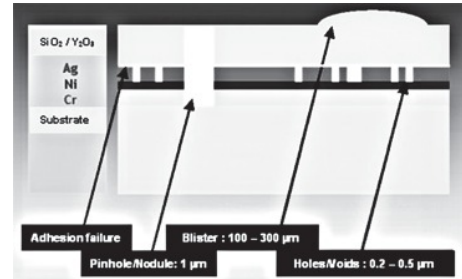


Fig. 2. Typical sample composition and morphological evolution of the typical materials with time.

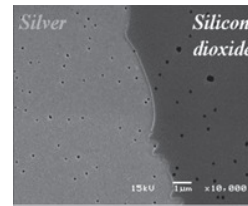


Fig. 3. A SEM picture of a sample surface (note the presence of holes in the silver film); on the left side of the sample, the SiO<sub>2</sub> protective film has been removed, which shows that holes appear within the silver thin film. (internal report [7]).

## 1.2. Aim of this study

Parameters such as temperature or atmosphere may enhance materials ageing as they stand either for kinetic or thermodynamic parameters. They are thus widely and commonly used in testing materials and specially bulk materials. In the case of materials under the form of thin films on a substrate, these techniques turn out to come close to their limits in the sense that they do not necessarily reproduce and speed up the spontaneous ageing of the materials. For instance, thin films systems behave differently according to their relative dimensions and/or intrinsic stress (resulting from out of equilibrium condensation).

In our case, the whole manufacturing process has been engineered to keep temperature of the device below 150°C : higher temperature would otherwise compromise system performances. Hence one cannot

rely on large temperature excursion to accelerate ageing phenomena. We believe that other acceleration factors can be found in stresses, provided one can modify the stress level in the multilayer. Our aim was to design an apparatus in which temperature, stress and gaseous atmosphere can be separately applied and monitored: a furnace-integrated four-point bending equipment.

Since generated stress fields have two origins: thermal (caused by heating and differences in the thermal expansion coefficients of the films and substrate) and mechanical (directly caused by the bending moment), it is necessary to plan concurrent experiments to derive thin film parameters from two other methods:

- Elastic modulus is one of the important material parameters, notably used in thin films technology for calculation of thermal stresses and stresses caused by the deformation imposed on the film when the component is loaded (or, vice versa, for assessment of deformations). Nanoindentation is one of the methods for determination of elastic modulus of thin films. This method is advantageous in that it has no special requirements regarding the specimen shape and preparation contrary to the bending of microbeams method.
- In addition to the exerted stress applied by four-point bending, thin films are subject to intrinsic or residual stress produced by preparation processes and developing during growth of the films. Virtually all deposited films are in a state of stress (all the more since deposition occur at low temperatures, that is to say far from equilibrium). The measurement of the intrinsic mechanical stress within the thin films will be achieved by means of the wafer curvature method which correlates the stress to the deflection of a strip coated on one side.

We will present here the first results obtained by these three techniques.

## 2. METHODOLOGY

### 2.1. Sample preparation

The geometrical features of real glass pieces used in scale 1 devices are not compatible with the selected experimental techniques. Hence we had to fabricate samples as close as possible to genuine mirrors, but capable of withstanding deformation large enough to be detected.

The coatings were deposited using a physical vapour deposition technique, that is electron beam (e-beam) evaporation. Because of the use of low expansion coefficient substrates in the case of real mirrors, the deposition process is performed at room temperature (< 100°C). All the materials were e-beam evaporated directly from a water-cooled copper multi-pocket

crucible. The box coater was cryopumped at under  $10^{-6}$  mbar ( $10^{-4}$  Pa) before deposition. The deposition rates were  $5 \text{ \AA} \cdot \text{min}^{-1}$ . In typical experiments, films were deposited onto  $5 \times 0.5 \times 0.05 \text{ cm}^3$  [111] silicon strips. To re-create a mirror-like interface a preliminary amorphous silicon dioxide film 30 nm in thickness was deposited. Samples intended for nanoindentation were deposited onto glass substrates 0.5 cm thick and 5 cm in diameter.

Monolayer specimens were used when properties of the films were specifically investigated whereas bilayer specimens were used to evaluate the global behaviour of mirror-like samples. In mono-layer specimens, films were grown until a 100 nm thickness was met while bilayer specimens were deposited as follows: 50 nm thickness for the underlayer (Ni or Cr) and 100 nm thickness for the upper layer (Ag). Using a multi-pocket crucible avoids subsequent venting between the deposition of each layer.

### 2.2. Methods and apparatus

#### 2.2.1 Ageing main experiment: 4-point bending under controlled heating and atmosphere

A dedicated apparatus allowing bending under thermal load (cf. Fig. 4 and Fig. 5) was constructed. Temperature and atmosphere controlling is provided by a furnace supplied with gas, vacuum system and heating controller while stress monitoring and application is provided by a four-point bending apparatus. The technique allows us to exert stress into a film on a substrate. Applied force is measured by means of an integrated force transducer and temperature by means of a thermocouple. Analogic signals are then digitalized and data are stored in a computer. The applied force is set from outside the furnace by mean of an hermetic micrometric screw which ensures the shift of the upper bearings and whose thread is known.

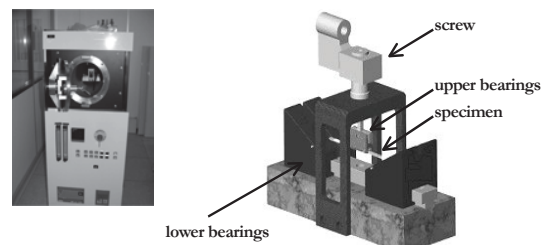


Fig. 4. (left) A picture of the ageing furnace equipped with the four-point bending apparatus; (right) The experimental apparatus for imposing strains by a four-point bending on films on substrates.

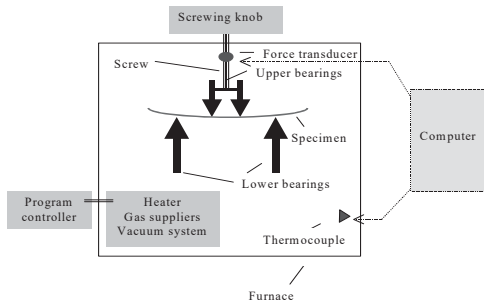


Fig. 5. Schematic of the integrated home-built apparatus with four-point bending capability.

The experimental procedure comprises the mounting of the sample, placement of the apparatus into the furnace, heating until the set temperature is reached, putting of the sample under bending *in situ* and time/force/temperature monitoring. Two additional reference samples are used: one is placed inside the furnace but without bending and the other outside in the ambient. Samples are observed by means of a microscope prior and after the experiment.

### 2.2.2. Measurement of intrinsic mechanical stress

Stresses in thin films on substrates are produced by processes which would cause the dimensions of the film to change if it were not attached to the substrate. If a film of thickness  $t_f$  having a biaxial stress  $\sigma$  is attached to a substrate of thickness  $t_s$ , it will cause the substrate to deform, as required by the condition of static equilibrium. If the substrate is significantly thicker than the film, the deformation will be spherical, having a radius of curvature  $R$ .  $R$  is determined by interferometry. The relationship between  $\sigma$  and  $R$  is given by the well-known Stoney [8] equation expressed as

$$\sigma = \frac{Y_s t_s^2}{6 t_f R} \quad (1)$$

where  $Y_s$  is the biaxial elastic modulus of the substrate (which is related to  $E_s$  Young's modulus, and  $\nu$ , Poisson's ratio for the substrate by

$$Y_s = \frac{E_s}{1 - 2\nu_s} \quad (2)$$

By convention, positive  $\sigma$  refers to a tensile stress state, in which the substrate is bent towards the film (concave), while negative  $\sigma$  corresponds to a compressive stress state, in which the substrate is bent away from the film (convex). Film stress was determined from the change in substrate's radius of curvature, before and after coating, using a Fizeau interferometer automated for curvature measurements of the substrate; the accuracy of the method is of the order of 30 nm as regards the deflection measurement

The sample is a 5x50 mm<sup>2</sup> {111}-oriented-Si substrate. As explained by Mirkarimi [9], the film stress  $\sigma$  can be calculated via a modified Stoney equation

$$\sigma = \frac{Y_s t_s^2}{6 t_f} \left( \frac{1}{R_2} - \frac{1}{R_1} \right) \quad (3)$$

where  $R_1$  and  $R_2$  are the radii of curvature of the substrate before and after coating. A value of 229 GPa for  $Y_s$  was used. We estimated that the stress measurements are accurate to  $\pm 10\%$ . In the case of a multilayer,  $t$  is taken as the total multilayer thickness.

### 2.2.3. Determination of mechanical properties of the thin films

In the case of thin films, nanoindentation [10] consists in investigating near surface regions of materials. The indenter penetrating into the materials deforms not only the film but usually also the substrate all the more as the loads are high. It is thus the composite (i.e. film + substrate) modulus, whose value is obtained in such a test, and the film modulus must be determined by a suitable data processing. In fact, with depth-sensing instruments, the elastic modulus is calculated by:

$$E^* = \frac{\sqrt{\pi}}{2} \frac{dP}{dh} \frac{1}{\sqrt{A}} \quad (4)$$

where  $A$  is the projected contact area (under load),  $dP/dh$  the slope of the load/displacement curve ( $P, h$ ) at the beginning of the unloading stage and  $E^*$  the "composite" modulus (couple "specimen + indenter"). Indeed, the elastic modulus is defined by the slope of the elastic zone of the rationalised 'load-strain' graph of a material. As far as nanoindentation is concerned, the so-called material is the couple "indenter + specimen". Evaluation is limited to the beginning of the unloading stage so as to ensure measurement in the elastic zone. During the loading stage, the material deforms elastically and plastically according to the load value. Since plastic deformations are permanent, unload is purely elastic.

Knowing the mechanical behaviour of the indenter, combination laws for mechanical properties allow us to access the specimen modulus  $E'$ .

$$\frac{1}{E^*} = \frac{1}{E'} + \frac{1}{E_i'} \quad (5)$$

$i$  refers to the indenter. Reduced modulus  $E'$  is used because the stress state in the contact zone is highly triaxial and comes with strong hydrostatic pressure due to lateral constraints. The elastic (Young) modulus is finally given by

$$E' = E / (1 - \nu^2) \quad (6)$$

where  $\nu$  represents the Poisson's ratio. Experimentally, the indentation procedure is as follows. All experiments were performed using the nanoindentation device UMIS 2000 at the Australian Technology Park

(Biomaterials Research Unit, The University of Sydney). A schematic illustration of the equipment is shown in Fig. 6.

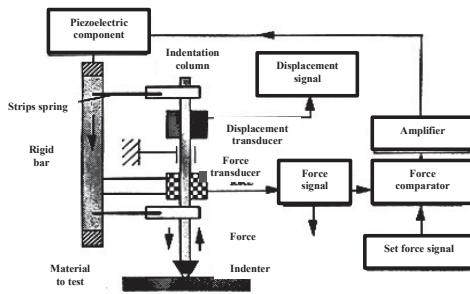


Fig. 6. A schematic diagram of the indentation operation. [from UMIS 2000 Operating Manual – CSIRO].

The system is a force-driven static measuring ultra micro-indentation instrument. It is force driven in the sense that the indenter is driven into the surface until a resistance equal to a set force is met. It is static measuring in the sense that penetration is measured under conditions of force equilibrium at each of a series of force steps. The elastic modulus is then derived from the load versus displacement data for an indentation experiment. The mode of operation which has been used is data acquisition by partial unload cycle, which enables to obtain modulus evaluations at each step of unloading and for various penetration depth. The tests were performed with nominal loads ranging from 0.25 to 5 mN (0,25; 0,5; 1; 5 mN). The nominal load ranges were divided in 20 intervals (incremented loads) and each experiment was repeated twice for 5 mN set force, three times for 1 mN set force and four times for 0,5 and 0,25 set forces so that averaged data could be used for each penetration force (that is for each increment). The experimental procedure for data acquisition was made up of successive steps as follows: zeroing of the system; achieving contact; force progression and unload cycles.

For data processing, the sample modulus were derived from the evaluated composite modulus. Data were the expressed and plotted as functions of the relative penetration  $a/t$ . The contact radius was calculated as  $a = h_c \tan \phi$ , where  $h_c$  is the measured contact depth of penetration, and  $\phi$  is the semiapical angle of the equivalent cone giving the same contact area as the Berkovich indenter for the same  $h_c$  ( $\phi \approx 70.3^\circ$ , for which  $a \approx 2.8 h_c$ ). the elastic modulus and Poisson's ratio of the indenter, used in the calculations, were taken from literature as:  $E_i = 1000 \text{ GPa}$ ,  $\nu_i = 0.2$ . Poisson's ratios of thin films were assumed to be equal to conventional bulk ratios. Data were then plotted for one film and regression functions were used to evaluate the film's modulus. Extrapolation towards high  $a/t$

represents the properties of the substrate (penetration much bigger than the film thickness) while  $a/t$  close to the y-axis ideally corresponds to the properties of the film (penetration near the surface region).

### 3. DATA & RESULTS

#### 3.1. SEM cross sections

The prepared samples are illustrated by the following SEM pictures taken at CNES/Toulouse (Fig. 7 and Fig. 8). One can note the columnar microstructure of the chromium film and the island microstructure of the silver film. Deposition onto nickel films is similar.

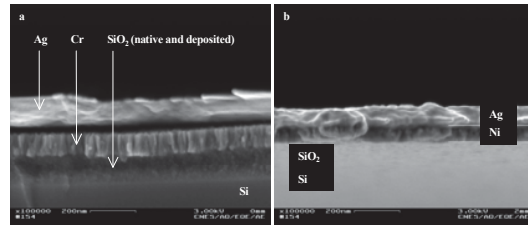


Fig. 7. Field-effect SEM cross-section image of  $\text{SiO}_2/\text{Cr}/\text{Ag}$  (a) and  $\text{SiO}_2/\text{Ni}/\text{Ag}$  (b) deposited onto Si. Magnification :  $\times 100\ 000$ .

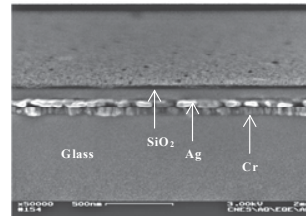


Fig. 8. Field effect SEM cross-section:  $\text{Cr}/\text{Ag}/\text{SiO}_2$  on glass. Magnification:  $\times 50\ 000$ .

#### 3.2. Wafer curvature measurements and related stress values

The residual stress measurement by the wafer curvature measurements gave the following residual stress evaluations.

Table 1. Intrinsic stresses of the layers	
Film material	Biaxial stress
$\text{SiO}_2$	- 50 MPa (compression)
Ag	+ 80 MPa (tension)
Cr	+ 700 MPa (tension)
Ni	+ 1400 (tension) [see*]
Cr/Ag (global)	+ 160 MPa (tension) measured + 250 MPa (tension) calculated
Cr/Ag/ $\text{SiO}_2$ (global)	+ 150 MPa (tension) measured + 150 MPa (tension) calculated

\* from a measurement reported in [J. TSAI *et al.*, *Thin Solid Films*, **365** (2000) 72–6] performed on a 60 nm Ni thin film on Si substrate (e-beam evaporated).

The global stress measured in the case of multilayer systems is in rather good agreement with the calculated value obtained by superposition principles (the global stress is obtained by adding together the individual stress contribution of each layer weighed by their respective thickness).

**3.3. Nanoindentation results**

For various reasons, such as irregular shape of the indenter tip and surface roughness (even of very smooth specimens), more reliable data are usually obtained for contact depths at least several tens of nanometers or more. With the exception of relatively thick coatings, the influence of the substrate cannot be neglected. The composite (film + substrate) modulus can generally be expressed as

$$E' = E'_s + (E'_f - E'_s)\phi(x) \tag{7}$$

where  $\phi$  is a certain (weight) function of relative penetration  $x$  (for instance  $a/t$ :  $a$  is the characteristic size (e.g. mean radius) of the contact area and  $t$  the film thickness).  $\phi = 1$  for zero penetration, and  $\phi \rightarrow 0$  for very large depths.

Modulus versus projected area-thickness ratio curves clearly show the influence of the substrate: at high  $a/t$  all measured modulus approach the substrate (B1664 type glass) modulus value. At lower  $a/t$ , that is when evaluation of the films is more actual, dispersion grow up. Regression functions were used to quantify the film modulus (Y-intercept) since Eq. 7 enables one to determine the film modulus  $E'_f$  from the  $E'$  values measured for one or more indenter loads and depths of penetration, provided the substrate modulus  $E'_s$  and the function  $\phi$  are known; this function is fitted to the experimental data, and  $E'_f$  is calculated as one of the regression constants. The results extracted from the curves are summarized in Table 2.

Table 2. Thin films elastic moduli.

Material	Modulus [GPa]
Ag	140
Cr	210
Ni	195
SiO <sub>2</sub>	60
Y <sub>2</sub> O <sub>3</sub>	125

**3.4. Ageing under mechanical stress: load by four-point bending**

The experiment was conducted in accordance with the following parameters:

- experiment duration: 22 hrs,
- set temperature: 45°C (which corresponds to a temperature difference of 25°C since deposition was carried at room temperature, that is 20°C),
- load: 1,2N corresponding to an edge penetration of 720 μm

- mounting: centred; upper bearings spacing: 1cm; lower bearings spacing: 3 cm,
- atmosphere: room air.

A finite elements calculus was performed with the help of the Navier equation [11] for structural mechanics. It enables to know the general shape of the stress distribution within a strip submitted to four-point bending (see Fig. 9 and Fig. 10).

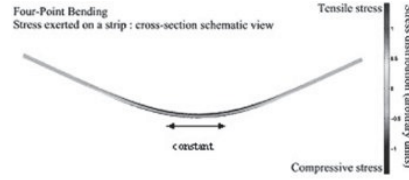


Fig. 9. (top) Schematic distribution within a specimen under four-point bending (finite elements) Tensile/compressive loads are allowed.



Fig. 10. Enlarged view of Fig. 9. Stress in central area is constant; it is under a gradient form towards the end.

Analytic calculus were performed to evaluate stress values in the central zone of each layer likely to be involved (see Fig. 12). These calculus are based on the theory of thin plates as developed in [12]. For the silver layer, the graph shows an additional stress of 100 MPa. In addition, stress due to thermal expansion differences\* between film and substrate is less than -9 MPa (compressive). It has been calculated in accordance with the thermal stress equation [13]

$$\sigma = -\frac{E}{1-\nu}(\alpha - \alpha_s)\Delta T. \tag{9}$$

\* thermal expansion coefficients: silver  $\alpha = 18.9 \cdot 10^{-6} \text{ K}^{-1}$ ; silicon  $\alpha_s = 3 \cdot 10^{-6} \text{ K}^{-1}$ ; E: silver Young modulus as determined by nanoindentation; silver Poisson's ratio:  $\nu = 0.38$  (bulk).

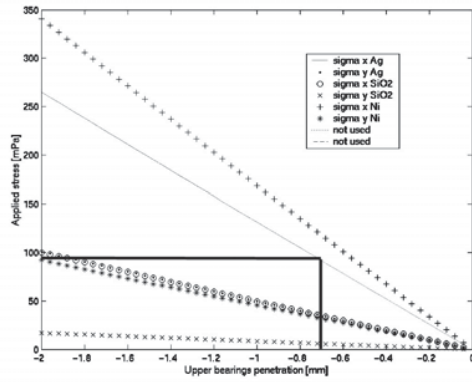


Fig. 11. Four-point bending: the applied stress (strip centre) vs. the wedge penetration for various films. (analytical calculus).

The following pictures (Fig. 12) clearly show the influence of stress in accelerated life tests for a given temperature.

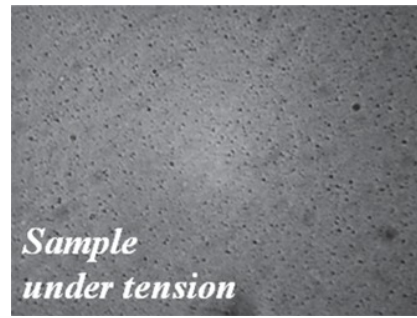
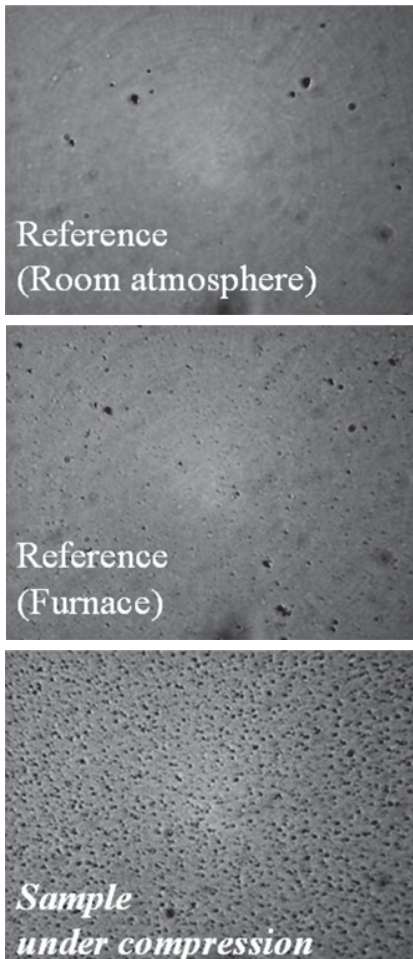


Fig. 12. Four micrographs of the specimens aged under various conditions, including stress application. Typical dimensions of the cavities : 0,1 – 0,2  $\mu\text{m}$ . [AGEING:  $t = 4 \text{ days}$ ;  $T_{\text{furnace}} = 50 \text{ }^\circ\text{C}$ ;  $F_{\text{applied}} = 8.5 \text{ N}$ ]

In the case of a standard ageing experiment, no relevant evolution is observed after 4 days at 50°C. Conversely, in the case stress is applied by means of four-point bending, an identical sample exhibits a clear evolution after 4 days at 50°C under 250 MPa compressive stress. Both density and size of the holes within the layer dramatically increased during the thermal and mechanical treatment. Even at such low temperatures, applying an external stress definitely revealed additional features compare to standard thermal treatment.

#### 4. DISCUSSION

Accelerated life tests including stress application are advantageous in several senses.

- They enable ageing without resorting to high temperatures, which prevents from damaging the specimens in a way they would not spontaneously.
- They do accelerate ageing as shown by the observations.
- They allow to point out the potential role played by stress in long-term ageing of the materials.

The observations are consistent with ageing models where internal stress play an important role. We believe that evolution with time, such as that observed at room temperature over rather long periods of times (several months to years) is most probably driven by stress within the thin films. Virtually all deposited films are in a state of stress, all the more since deposition is performed at low temperatures, out of equilibrium. The residual stress represents stored energy to be released by physicochemical processes whose purpose is to attain a more stable situation. This evolution is likely to give rise to ageing and degradation. In addition to that intrinsic phenomenon, during the storage stage, the multilayers are subject to environment conditions and variations, such as temperature changes, atmospheric water adsorption by the protective film [14], internal solid state reactions within or between layers (e.g. adhesion promoter). All

of these changes produce stress as they would cause the dimensions of the films to change if they were not attached to the substrate. Hence the multilayers will show additional ageing behaviour due to environment variations. The four-point bending ageing apparatus developed seems therefore to be capable of enhancing ageing phenomena as it increases either the available energy intrinsically stored within the films or reproduces over a short-term period stress developing with environment changes. It enables to reproduce natural ageing over a short period of time.

## 5. CONCLUSION

Ageing of silver-based mirrors was investigated. Preliminary required tests were performed and parameters such as residual stresses and elastic modulus are available. An accelerated life test based on bending under thermal load for exerting both temperature and strain on the thin films systems was successfully developed. Contrary to techniques consisting only in heating, exerting concurrently additional stress resulted in clear accelerated ageing. Stress-induced voiding kinetics was enhanced. This technique appears to be capable of enhancing ageing and evaluating the role of stress. Tests under various atmospheres for determining more precisely physicochemical processes involved will soon be performed and stress-induced voiding simulations and statistical calculus applied to our case are under progress.

## ACKNOWLEDGMENT

We wish to thank Laurent Debove and Charles Josserond (INPG/CNRS) for their primordial involvement in designing, building and installing the new apparatus. We gratefully acknowledge the support for the SEM pictures by Vanessa Chazal (CNES). We would also thank Viviane Muffato and Christelle Anglade (CEA/Léti) for assistance with samples preparation and Olivier Lartigue (CEA/Léti) for assistance with samples observations. We are grateful to Mikhail Mamatkoulov (Université Joseph-Fourier) for support with calculus methods.

## REFERENCES

1. D. HULL, D. E. RIMMER, "The growth of grain-boundary voids under stress", *Philosophical Magazine*, **4**, pp. 673–87, 1959.
2. A. E. B. PRESLAND, G. L. PRICE, D. L. TRIMM, "Hillock formation by surface diffusion on thin silver films", *Surface Science*, **29**, 1971.
3. A. E. B. PRESLAND, G. L. PRICE, D. L. TRIMM, "The role of microstructure and surface energy in hole growth and island formation in thin

- silver films", *Surface Science*, **29**, pp. 435–46, 1971.
4. L. SCHMIRGELD-MIGNOT, P. J. A. MOLINÀS-MATA, S. POISSONNET, G. MARTIN, "Reactive solid-state dewetting", *Philosophical Magazine Letters*, **80** (1), pp. 33–40, 2000.
5. H. DE MONESTROL, L. SCHMIRGELD-MIGNOT, P. J. A. MOLINÀS-MATA, S. POISSONNET, G. MARTIN, "Kinetics and mechanisms of reactive solid state dewetting in the system Ag–Ni–O", *Acta Materialia*, pp. 1655–60, **49**, 2001.
6. S. KOMI, M. FUKUI, Y. SHINTANI, "Aging histories of optical constants of thermally evaporated silver and copper films", *Surface Science*, **237**, pp. 321–6, 1990.
7. G. RAVEL, E. QUESNEL, C. PELLÉ, F. BAUME, "Étude des argentures – Rapport CEA/CNES", *Internal report CEA* (note published), 2000.
8. G.G. STONEY, "The tension of metallic films deposited by electrolysis", *Proc. R. Soc. Lond.*, pp.172–5, 1909.
9. P.B. MIRKARIMI, "Stress, reflectance, and temporal stability of sputter-deposited Mo/Si and Mo/Be multilayer films for EUV lithography", *Optical Engineering*, **38** (7), pp. 1246–59, 1999.
10. J. MENČIK, D. MUNZ, E. QUANDT, E. R. WEPPELMANN, M. V. SWAIN, "Determination of elastic modulus of thin layers using nanoindentation", *Journal of Materials Research*, 2003 (to be published).
11. L. LANDAU, E. LIFCHITZ, *Théorie de l'élasticité*, 2<sup>ème</sup> édition, p. 31, Éd. Librairie du Globe – Mir, Moscow, 1987.
12. P. SCAFIDI, M. IGNAT, M. DUPEUX, "Mechanical stability of passivation films deposited on aluminium substrates", *Materials Reliability in Microelectronics III*, Materials Research Society Symposium Proceedings, 309, p. 55, MRS, 1993.
13. W. BRÜCKNER, S. BAUNACK, "Stress and oxidation in CuNi thin films", *Thin Solid Films*, **355–356**, pp. 316–21, 1999.
14. H. LEPLAN, J. Y. ROBIC, Y. PAULEAU, "Kinetics of residual stress evolution in evaporated silicon dioxide films exposed to room air", *Journal of Applied Physics*, **79** (9), pp. 6926–31, 1996